

## Supporting Information

### Developing visible-light-induced dynamic aromatic Schiff base bonds for room-temperature self-healable and reprocessable waterborne polyurethanes with high mechanical properties

Wuhou Fan <sup>a,b,c</sup>, Yong Jin <sup>a,b\*</sup>, Liangjie Shi <sup>a,b</sup>, Rong Zhou<sup>a,b</sup> and Weining Du <sup>a,b</sup>

<sup>a</sup> National Engineering Laboratory for Clean Technology of Leather Manufacture, Sichuan University, No. 24 South Section 1, Yihuan Road, Chengdu, 610065, China

<sup>b</sup> The Key Laboratory of Leather Chemistry and Engineering of Ministry of Education, Sichuan University, No. 24 South Section 1, Yihuan Road, Chengdu, 610065, China

<sup>c</sup> High-tech Organic Fibers Key Laboratory of Sichuan Province, Sichuan Textile Scientific Research Institute, No. 2, Twelve Bridge Road, Chengdu, 610072, China

\*To whom correspondence should be addressed. E-mail: jinyong@cioc.ac.cn;

#### Experimental Section

##### Synthesis of bis(4-hydroxyphenyl) (methylenebis(4,1-phenylene))dicarbamate (DiAU-DiOH)

1,4-Dihydroxybenzene (11.01 g, 0.1 mol) dissolved in 50 mL of DMF was fed in a flask (100 mL) equipped with a reflux condenser device under the protection of nitrogen, and then a drop of DBTL was added. Subsequently, 4,4'-diphenylmethane diisocyanate (12.51 g, 0.05 mol) dissolved in 50 mL of DMF was fed dropwise, and the reaction was kept at 80°C for 8 hours. After cooling to room temperature slowly, the reactant was poured into a 1 000 mL of absolute ethyl ether and a large amount of white precipitate appears. The crude product was filtered and washed with acetone for three times, and dried at 60 °C at a vacuum degree of -0.09 MPa, respectively, to obtain a white solid of DiAU-DiOH with a yield of 98.0%. <sup>1</sup>H-NMR (400MHz, *d*<sub>6</sub>-DMSO):  $\delta$  (ppm) = 10.03 (-OH), 9.43 (HNC=O), 3.82 (C-H of methylene), 6.74-7.38 (Ar-H) (Fig. S3).<sup>1,2</sup> FTIR (KBr, cm<sup>-1</sup>): 3329.1 ( $\nu$ (N-H)), 1720.8 ( $\nu$ (C=O)), 1602.8, 1506.4, and 1458.2 ( $\nu$ (C=C) of phenyl groups), 1541.1 ( $\delta$ (N-H)), 1228.7 ( $\nu$ (C-N)), 1192.0 ( $\nu$ (C-O)), 814.0 ( $\gamma$ (C-H) of phenyl groups) (Fig. S4).<sup>1,2</sup>

##### Synthesis of N-(4-methylbenzylidene)-3-chloroaniline (ASB-2)

The synthesis of ASB-2 was according to the method mentioned by akhter et al.<sup>3</sup> *p*-Methyl benzaldehyde (6.01g, 0.01 mol) dissolved in 100 mL of anhydrous ethanol was fed in a flask (250 mL) equipped with a reflux condenser device under the protection of nitrogen. Subsequently, *p*-chlorophenylamine (6.38g, 0.05 mol) dissolved in 50 mL of anhydrous ethanol was fed dropwise,

and the reaction was refluxed for 8 hours. After cooling to room temperature slowly, the crude product was filtered, dried and recrystallized from ethanol, respectively, to obtain a yellow solid of ASB-2 with a yield of 80.1%. <sup>1</sup>H-NMR (*d*<sub>6</sub>-DMSO):  $\delta$  (ppm) = 8.58 (*HC=N*), 7.27-7.82 (*Ar-H*), 2.38 (*-CH<sub>3</sub>*) (Fig. S9b).<sup>1,2</sup>

### Synthesis of N-(4-methylbenzylidene) aniline (ASB-3)

The synthesis of ASB-2 was according to the method mentioned by akhter et al.<sup>3</sup> *p*-Methyl benzaldehyde (6.01g, 0.01 mol) dissolved in 100 mL of anhydrous ethanol was fed in a flask (250 mL) equipped with a reflux condenser device under the protection of nitrogen. Subsequently, phenylamine (4.65g, 0.05 mol) dissolved in 50 mL of anhydrous ethanol was fed dropwise, and the reaction was refluxed for 8 hours. After cooling to room temperature slowly, the crude product was filtered, dried and recrystallized from ethanol, respectively, to obtain a yellow solid of ASB-3 with a yield of 82.5%. <sup>1</sup>H-NMR (*d*<sub>6</sub>-DMSO):  $\delta$  (ppm) = 8.57 (*HC=N*), 7.24-7.83 (*Ar-H*), 2.38 (*-CH<sub>3</sub>*) (Fig. S9c).<sup>1,2</sup>

### Synthesis of N-benzylidene-4-chloroaniline (ASB-4)

The synthesis of ASB-2 was according to the method mentioned by akhter et al.<sup>3</sup> Benzaldehyde (5.31g, 0.01 mol) dissolved in 100 mL of anhydrous ethanol was fed in a flask (250 mL) equipped with a reflux condenser device under the protection of nitrogen. Subsequently, *p*-chlorophenylamine (6.38g, 0.05 mol) dissolved in 50 mL of anhydrous ethanol was fed dropwise, and the reaction was refluxed for 8 hours. After cooling to room temperature slowly, the crude product was filtered, dried and recrystallized from ethanol, respectively, to obtain a yellow solid of ASB-4 with a yield of 83.2%. <sup>1</sup>H-NMR (*d*<sub>6</sub>-DMSO):  $\delta$  (ppm) = 8.64 (*HC=N*), 7.28-7.92 (*Ar-H*) (Fig. S9d).<sup>1,2</sup>

### The standard di-n-butylamine back-titration

After the addition of DiASB-DiOH, the reaction process was monitored by the standard di-n-butylamine back-titration method to determine the endpoint of prepolymerization reaction.<sup>4,5</sup> The theoretical NCO content of ASB-WPU prepolymer ( $w_1$ ) was calculated using the following equation:

$$w_1(\%) = \frac{(N_{IPDI} - N_{PTMG} - N_{DMPA} - N_{BDO} - N_{DiASB-DiOH}) \times 2 \times M_{NCO}}{m_{IPDI} + m_{PTMG} + m_{DMPA} + m_{BDO} + m_{DiASB-DiOH} + m_{butanone}} \times 100\%$$

(1)

where  $N_{IPDI}$ ,  $N_{PTMG}$ ,  $N_{DMPA}$ ,  $N_{BDO}$  and  $N_{DiASB-DiOH}$  represent the mole number of IPDI, PTMG, DMPA, BDO, and DiASB-DiOH, respectively. Meanwhile,  $m_{IPDI}$ ,  $m_{PTMG}$ ,  $m_{DMPA}$ ,  $m_{BDO}$ ,  $m_{DiASB-DiOH}$  and  $m_{butanone}$  represent the mass of IPDI, PTMG, DMPA, BDO, DiASB-DiOH, and butanone, respectively.  $M_{NCO}$  is the molar mass of NCO group (42.02 g/mol). The calculated theoretical NCO content ( $w_1$ ) of ASB-WPU prepolymer is 0.65%.

After the addition of DiASB-DiOH and reacted at 80°C for 5 hours, approximately 1.0 g of ASB-WPU prepolymer was sampled and dissolved in 25 mL of toluene. After the complete dissolution of prepolymer, 25 mL of toluene-dibutylamine solution (0.1 mol/L) was added and stirred for 10 minutes. After placed for 30 minutes, 100 mL of isopropanol and several drops of bromocresol green indicator was added, and the solution was titrated with HCl standard solution (0.1 mol/L). When the tipping point is coming, the color of the solution changes from green to yellow, and the consumption of HCl solution was record. Furthermore, the blank experiment was also carried out. The tested NCO content of sampled ASB-WPU prepolymers ( $w_2$ ) was calculated using the following equation:

$$w_2(\%) = \frac{(V_0 - V_1) \times C_{HCl} \times M_{NCO}}{m_{prepolymer}} \times 100\% \quad (2)$$

where  $m_{prepolymer}$  represents the mass of sampled ASB-WPU prepolymer with terminated NCO groups,  $M_{NCO}$  is the molar mass of NCO group (42.02 g/mol), and  $C_{HCl}$  is the concentration (0.1 mol/L) of HCl solution, respectively. Meanwhile,  $V_0$  and  $V_1$  represent the volume of HCl solution consumed in the titration of the blank sample excludes NCO-terminated ASB-WPU prepolymers and NCO-terminated prepolymers, respectively.

After the addition of DiASB-DiOH and reacted at 80°C for 5 hours, the value of  $w_2$  for the representative ASB-WPU-2 prepolymer was 0.66%, which is close to the theoretical value of  $w_1$  (0.65%), which indicates that DiASB-DiOH was almost reacted with the NCO groups and the dynamic ASB bonds were successfully introduced into the polymer chain of ASB-WPU-2 prepolymer.

## Characterization

**Nuclear Magnetic Resonance Spectroscopy (NMR):** The  $^1\text{H}$ -NMR spectra was determined on a JNM-ECA 300 Spectrometer (JEOL, Japan) with  $\text{CDCl}_3$  or  $\text{d}_6$ -DMSO as a solvent at 300 MHz.

**Fourier Transform Infrared (FTIR) spectra:** The FTIR spectra were recorded using an IRAffinity-1 FTIR spectrometer (Shimadzu, Japan) with a resolution of  $4 \text{ cm}^{-1}$  over a spectral range of 400 to  $4000 \text{ cm}^{-1}$  at 25°C.

**Gel permeation chromatography (GPC):** GPC measurement was conducted on a Breeze2 (Waters, USA) using polystyrene as a standard and tetrahydrofuran as an eluent (flow rate: 1.0 mL/min, at 40 °C).

**Transmission Electron Microscopy (TEM):** Morphology of emulsion particles was observed using a H7650 transmission electron microscopy (Hitachi, Japan) with an accelerating voltage of 75 kV and the sample was stained by 0.2 wt % phosphotungstic acid hydrate before observation.

**Dynamic Light Scattering (DLS):** Particle size of the obtained emulsion was determined using a Nano S90 Dynamic Light Scattering (DLS) analyzer (Malvern, UK) at 25°C, and the results were the mean value of three measurements.

**UV/Vis Transmittance Spectrometer:** Transmittance of film samples with a thickness of  $\sim 100$

$\mu\text{m}$  was determined by a SP-756P UV/Vis spectrometer (Spectrum, China) in the wavelength range of 380 to 780 nm at 25°C.

**UV/Vis Absorption Spectrometer:** Absorption of DiASB-DiOH was determined by a SP-756P UV/Vis spectrometer (Spectrum, China) in the wavelength range of 380 to 780 nm at 25°C, with a concentration of 0.005 mol/L in ethanol.

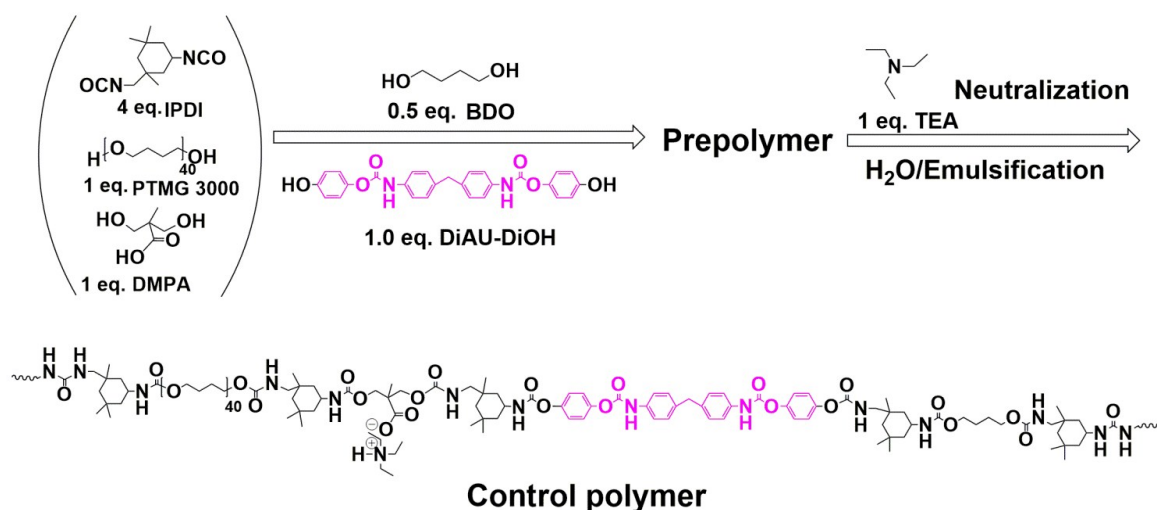
**Dynamic Mechanical Analysis (DMA):** DMA curves were obtained on a DMA 242C (Netzsch, Germany) in the tensile resonant mode, at a heating rate of 5 K/min from -90 °C to 90 °C. The loss factor ( $\tan \delta$ ) was obtained at 1 Hz frequency.

**Differential Scanning Calorimetry (DSC):** DSC tests were conducted by a DSC 204F1 apparatus (Netzsch, Germany) with a range of 25 to 240°C by a heating ratio of 10 °C/min, and a heat cycle was conducted firstly to eliminate the thermal history.

**X-Ray Diffraction (XRD):** XRD patterns were determined on an X'Pert Pro MPD DY129 diffractometer (Panalytical, Holland) using  $\text{CuK}\alpha$  radiation ( $\lambda = 1.541 \text{ \AA}$ ). Each sample was recorded at a scanning rate of 4°/min in the  $2\theta$  range from 10° to 80°.

**Thermo-Gravimetric Analysis (TGA):** TGA was performed on a STA 449F3 (Netzsch, Germany). Each sample was heated at a rate of 10 K/min from 30 °C to 480 °C under nitrogen atmosphere.

**Stress-Strain Tests:** The strain-stress tests were conducted by a UTM 6203 electronic universal tester (SUNS, China) with a 2 KN load cell at a cross-head speed of 50 mm  $\text{min}^{-1}$  at room temperature. The tested samples were tailored into an oblong shape with a length of 30 mm, a width of 5 mm and a thickness of  $\sim 1.5$  mm. Mechanical properties including ultimate tensile stress and elongation at break were obtained and the results were the mean values of five measurements. Toughness, which is defined as the area surrounded by the tensile stress-strain curve, was also calculated by using the software of Origin Pro 9.0 and its value were the mean values of five times.



**Scheme S1.** Synthesis of the control polymer.

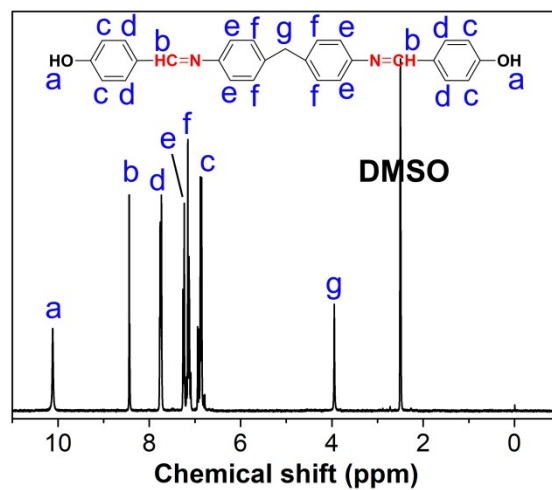


Fig. S1. <sup>1</sup>H-NMR spectrum of DiASB-DiOH.

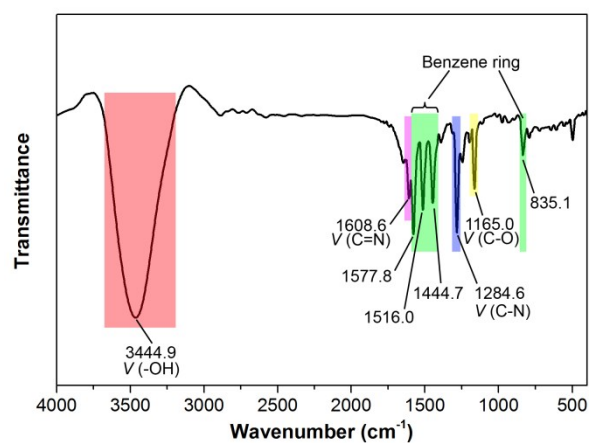


Fig. S2. FTIR spectrum of DiASB-DiOH.

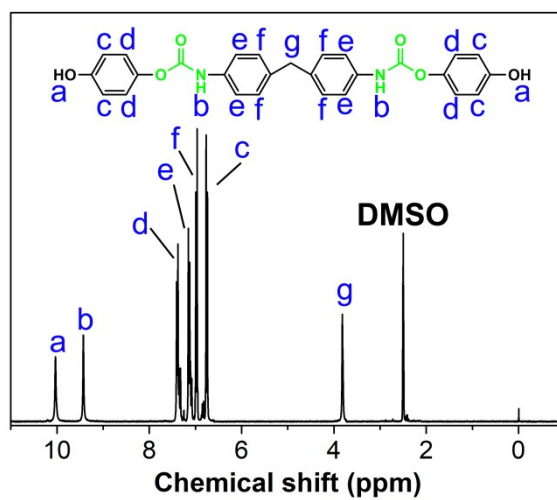


Fig. S3. <sup>1</sup>H-NMR spectrum of DiAU-DiOH.

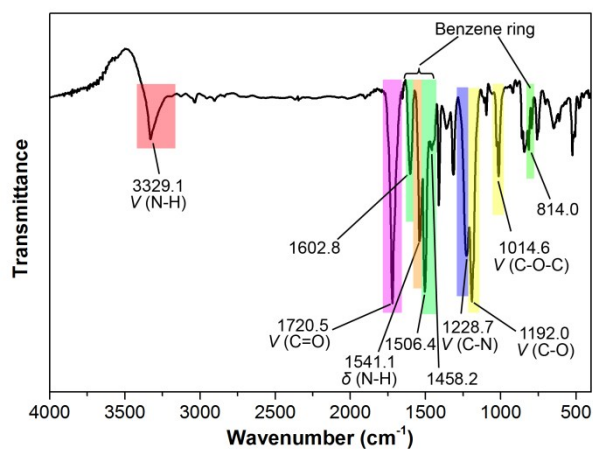


Fig. S4. FTIR spectrum of DiAU-DiOH.

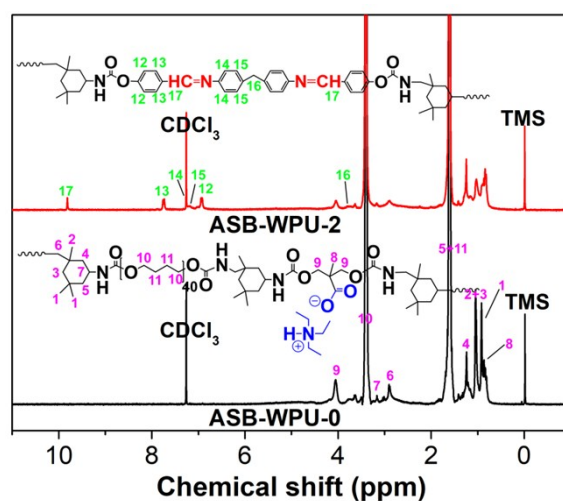


Fig. S5. <sup>1</sup>H-NMR spectrum of ASB-WPU-0 and ASB-WPU-2.

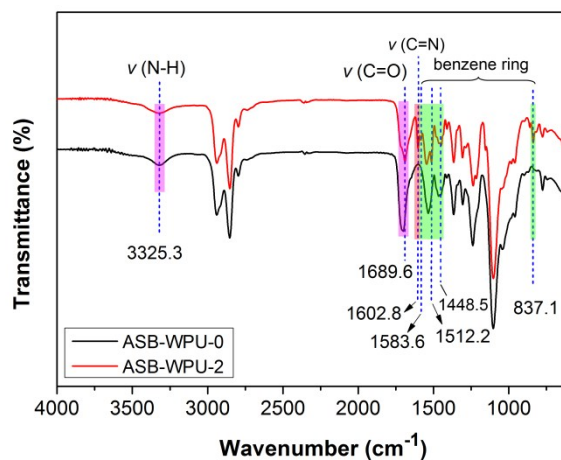
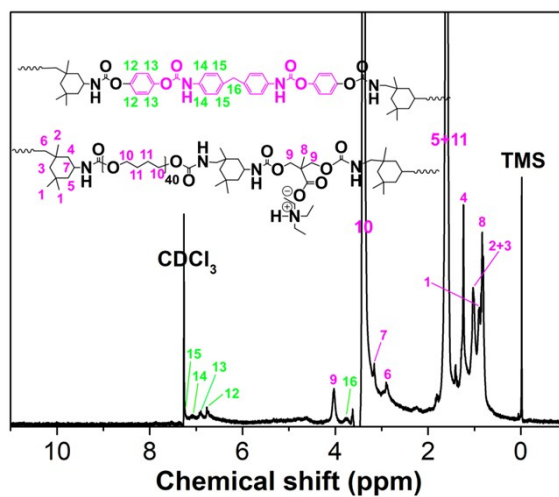
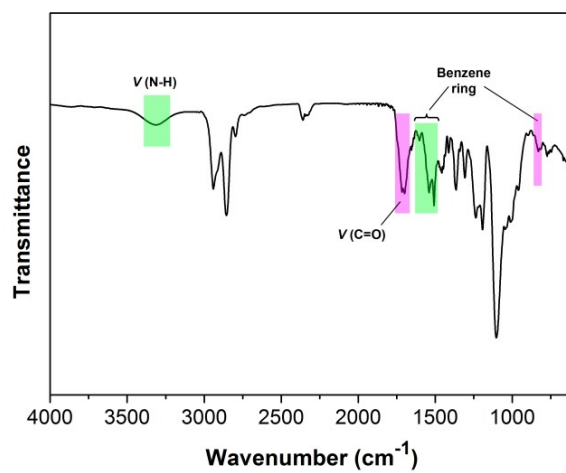


Fig. S6. FTIR spectrum of ASB-WPU-0 and ASB-WPU-2.



**Fig. S7.**  $^1\text{H-NMR}$  spectrum of the control polymer.



**Fig. S8.** FTIR spectrum of the control polymer.

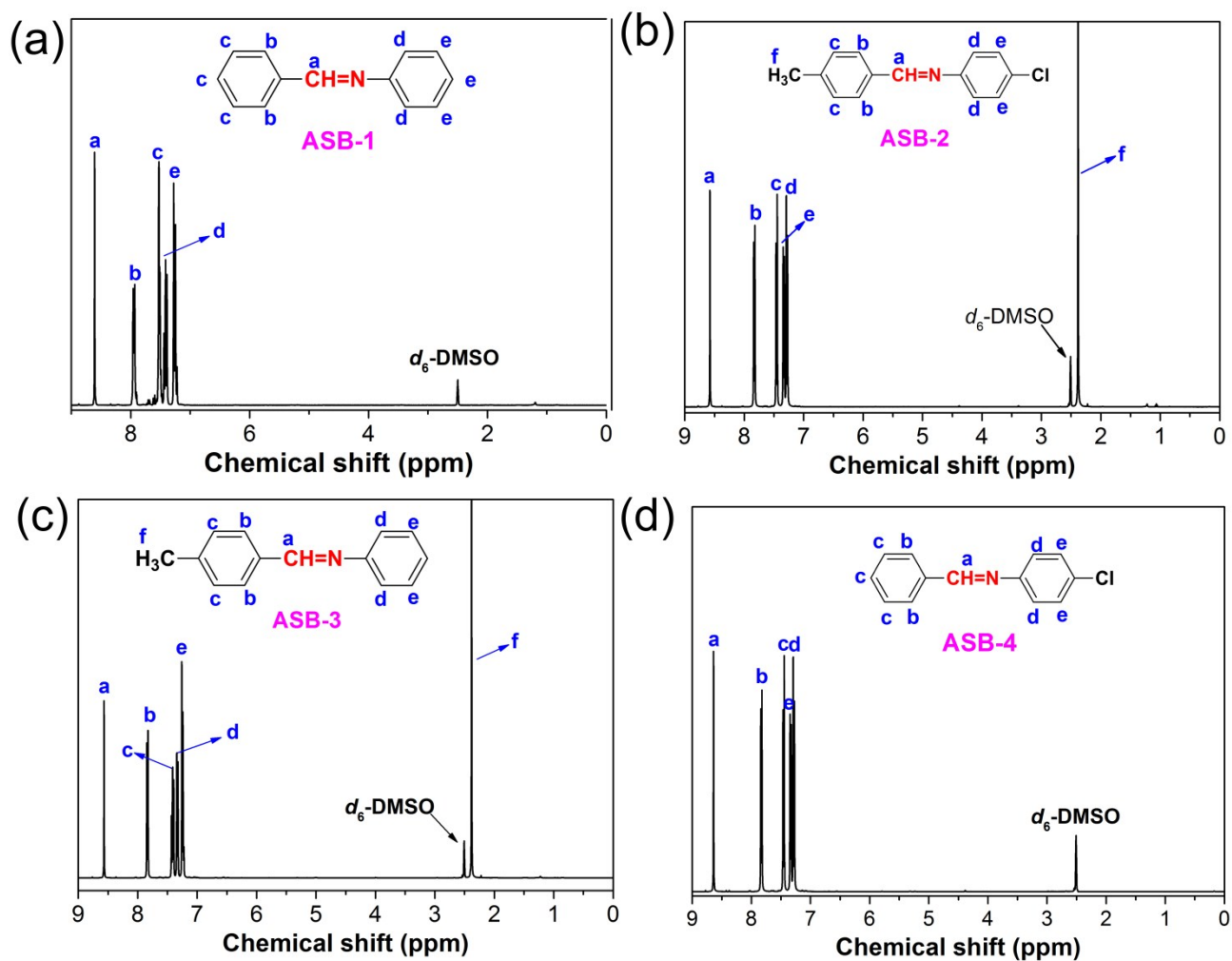


**Fig. S9.**  $^1\text{H}$ -NMR spectrum of (a) ASB-1) (b) ASB-2, (c) ASB-3 and (d) ASB-4. ASB-1 (400MHz,  $d_6$ -DMSO):  $\delta$  (ppm) = 8.62 ( $\text{HC}=\text{N}$ ), 7.28-7.93 ( $\text{Ar-H}$ ).

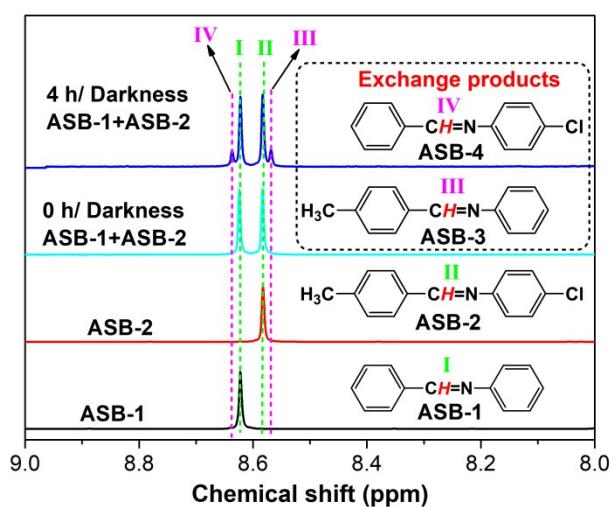


**Fig. S10.**  $^1\text{H}$ -NMR spectrum of the exchange products of an equivalent amount (0.005 mol/L) of ASB-1 and ASB-2 in  $d_6$ -DMSO in the chemical shift ranged from 8.0 to 9.0 ppm after placed in darkness for 4 hours.

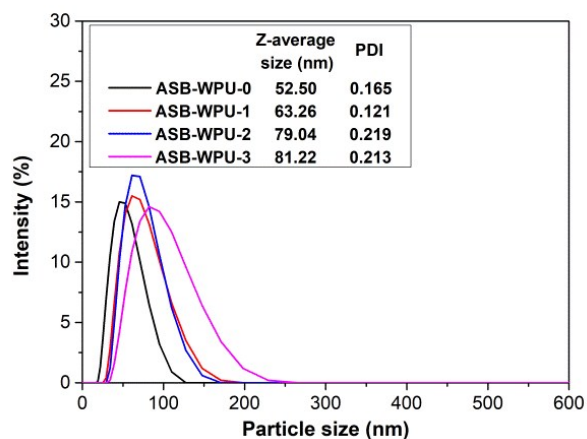


**Fig. S11.** Particle size distribution of ASB-WPU emulsions.

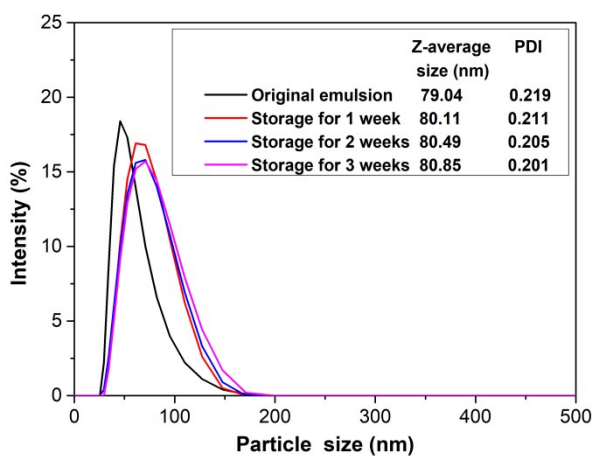


**Fig. S12.** Particle size distribution of ASB-WPU-2 emulsions with different storage time.

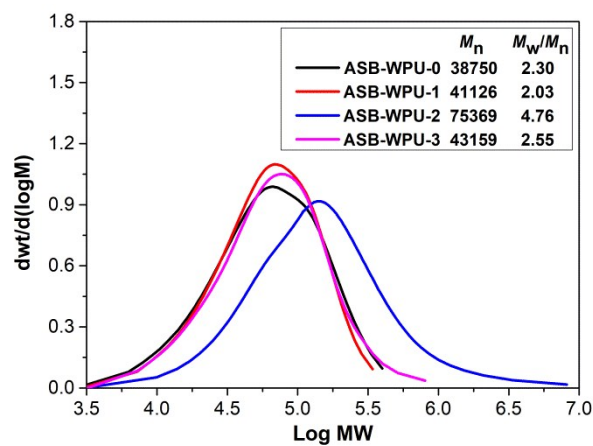


**Fig. S13.** GPC curves of ASB-WPU polymers.

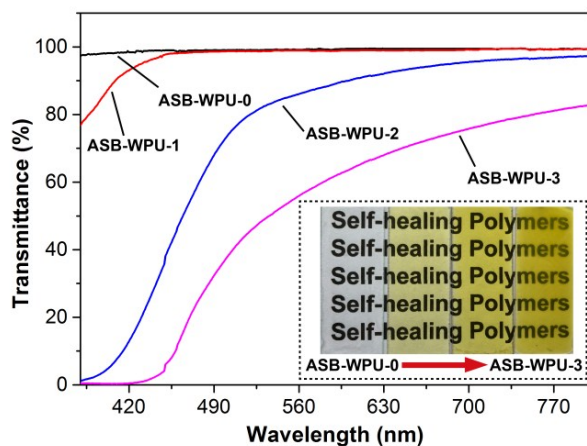


Fig. S14. Transmittance of ASB-WPU films in the visible light region.

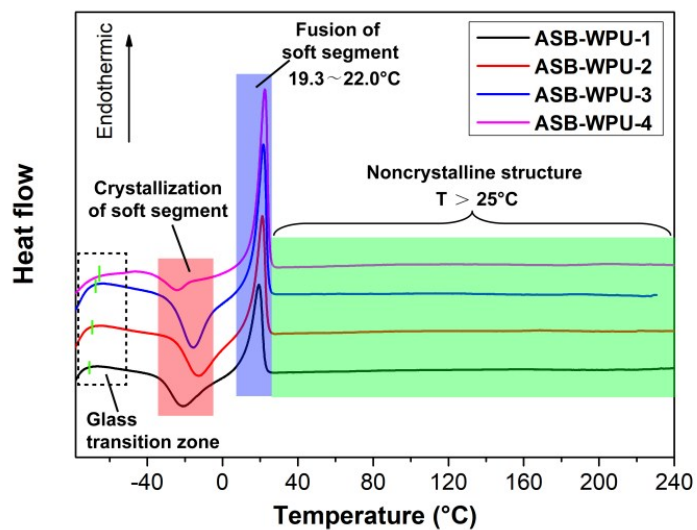


Fig. S15. DSC curves of ASB-WPU films.

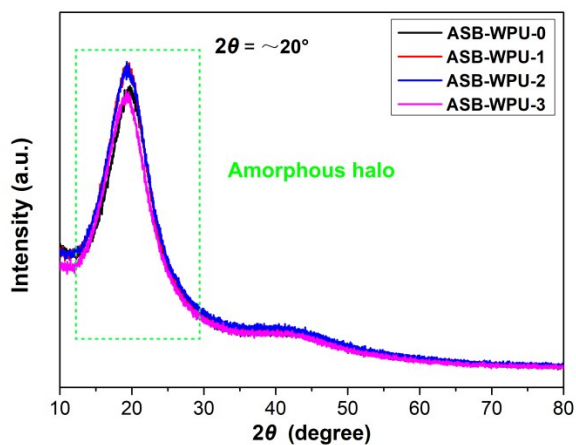
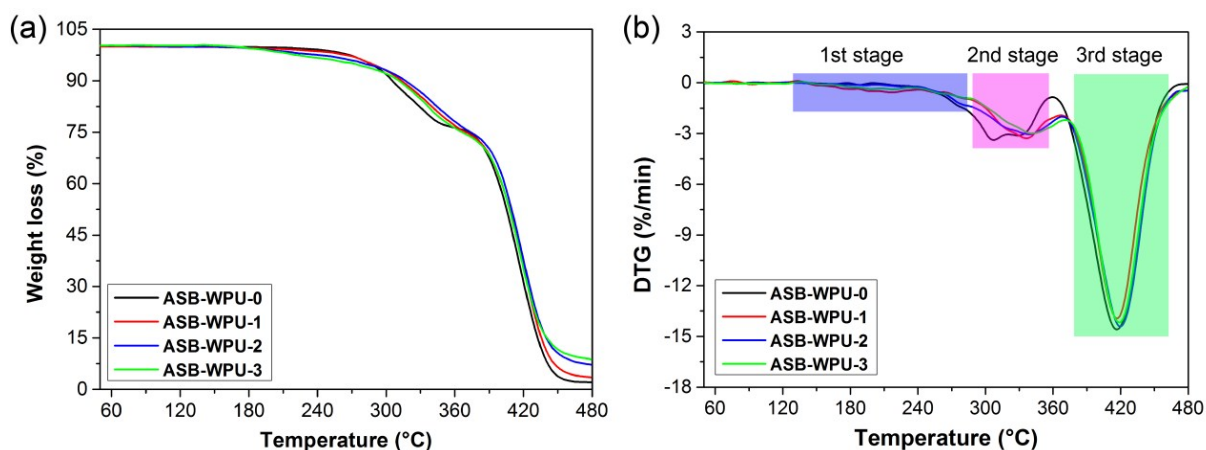


Fig. S16. XRD curves of ASB-WPU films.



**Fig. S17.** TGA and DTG curves of ASB-WPU films in the temperature ranges from 50°C to 480°C: (a) TGA curves, (b) DTG curves.

**Table S1. Thermal properties of ASB-WPU polymers**

| Sample code | $T_{5\%}$ (°C) | $T_{max^2}$ (°C) | $T_{max^3}$ (°C) | Residual rate (%) |
|-------------|----------------|------------------|------------------|-------------------|
| ASB-WPU-0   | 272.0          | 306.2            | 416.3            | 2.08              |
| ASB-WPU-1   | 281.0          | 337.1            | 417.1            | 3.49              |
| ASB-WPU-2   | 286.0          | 337.6            | 419.2            | 7.21              |
| ASB-WPU-3   | 287.0          | 341.1            | 419.6            | 8.77              |

**Note:**  $T_{5\%}$ ,  $T_{max^2}$  and  $T_{max^3}$  represent the temperature at mass loss of 5.0 wt%, the temperature at the maximum decomposition rate of the second stage, and the temperature at the maximum decomposition rate of the third stage, respectively.

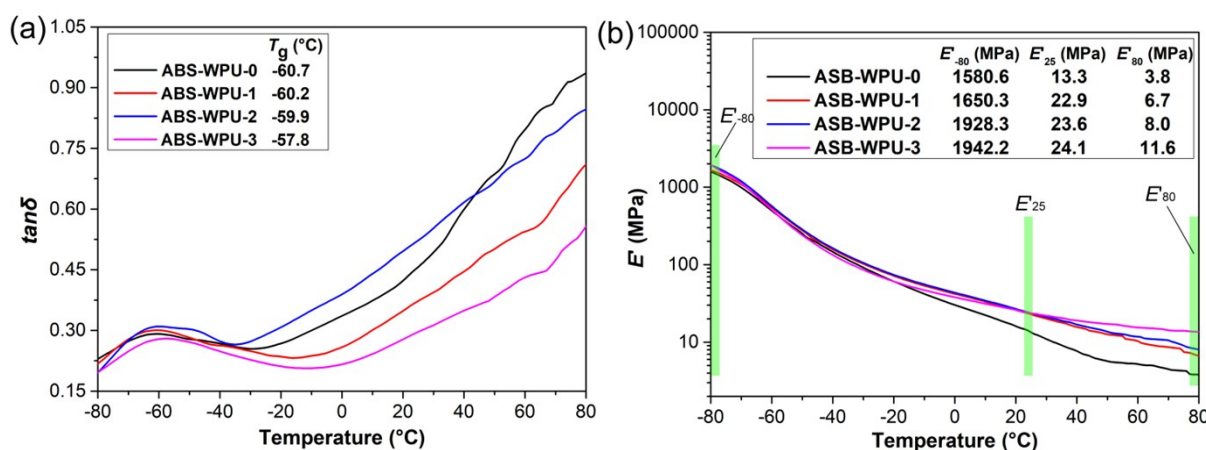


**Fig. S18.** DMA curves of ASB-WPU films in the temperature ranges from -80°C to 80°C: (a)  $\tan\delta$ , (b) storage modulus ( $E'$ ).

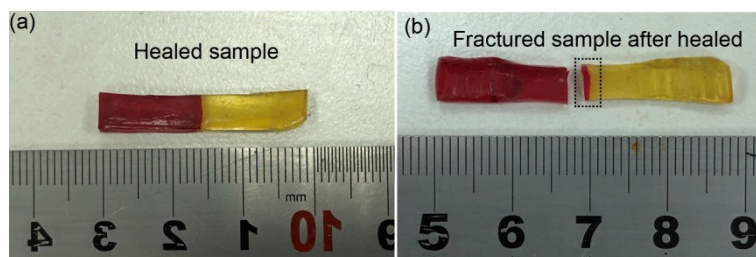


**Fig. S19.** Photographs of the healed ASB-WPU-2 specimen (a) before and (b) after the stress-strain tests.

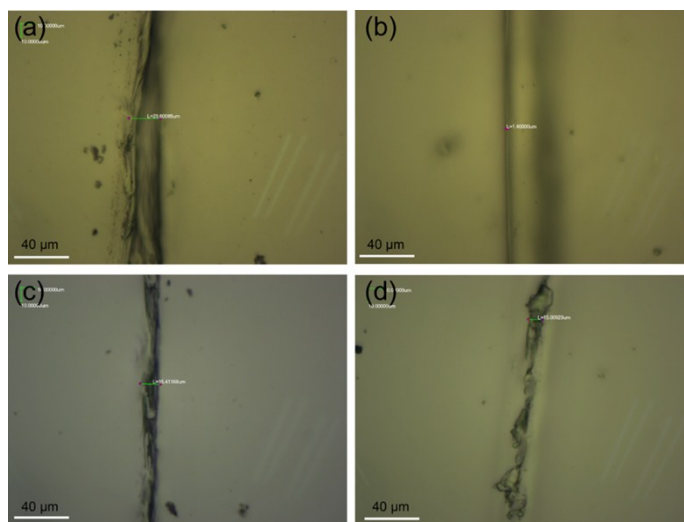


**Fig. S20.** Optical microscopy images of the fractured ASB-WPU-2 sample (a) before and (b) after healed in darkness for 24 hours at 25°C, and the fractured control samples (c) before and (d) after healed under visible light for 24 hours at 25°C.

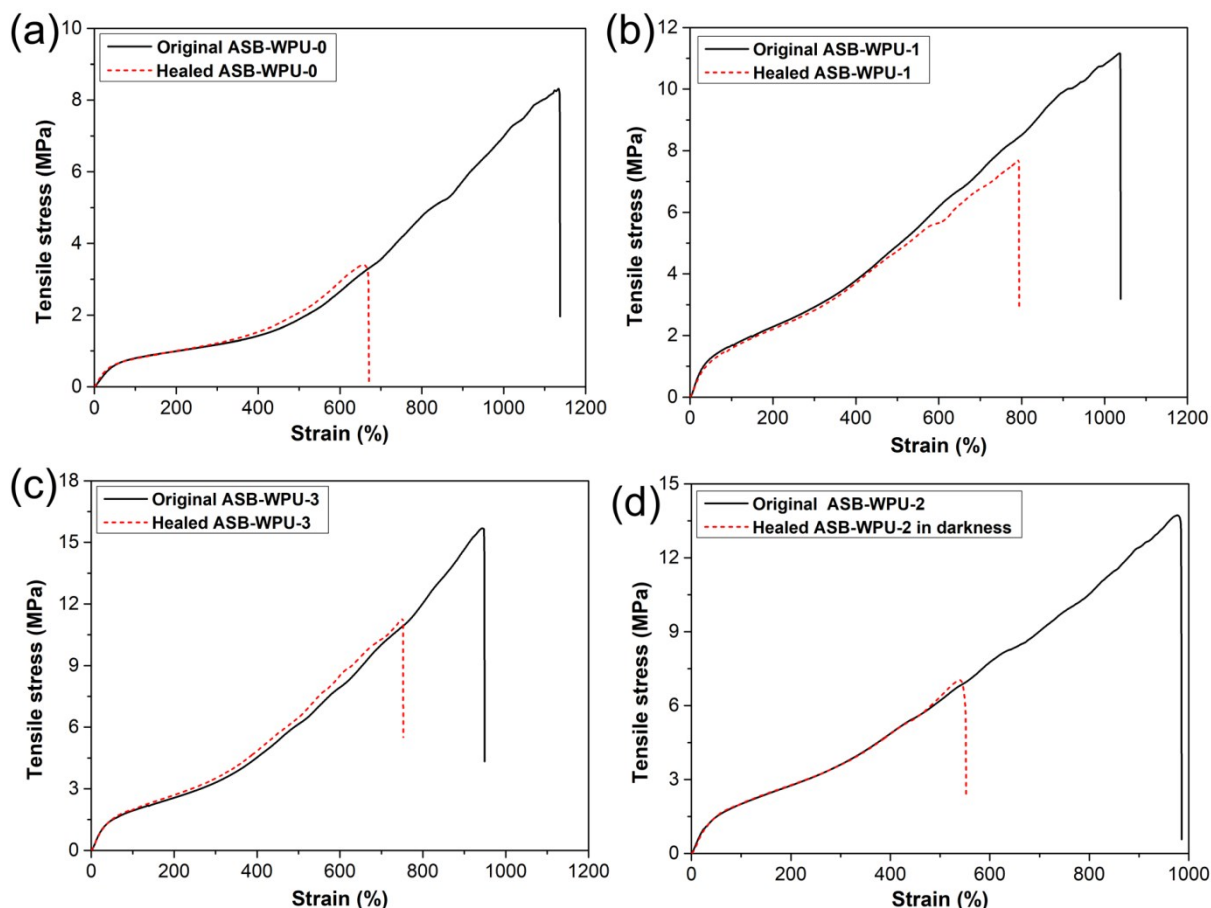


**Fig. S21.** Stress-strain curves of the healed ASB-WPU specimens: (a) ASB-WPU-0 healed under visible light for 24 hours; (b) ASB-WPU-1 healed under visible light for 24 hours; (c) ASB-WPU-3 healed under visible light for 24 hours; (d) ASB-WPU-2 healed in darkness for 24 hours.

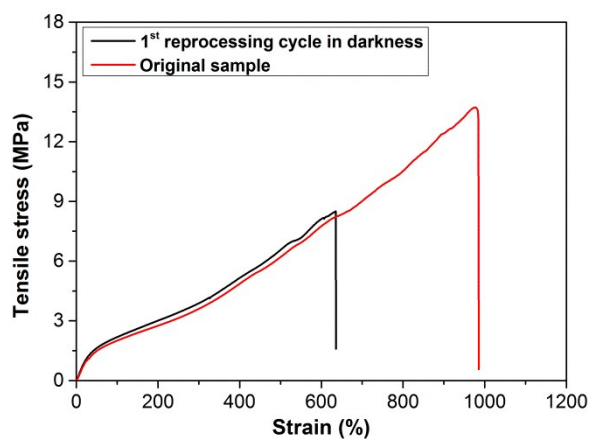


**Fig. S22.** Stress-strain curves of ASB-WPU-2 polymer grains after reprocessed in darkness for 48 hours.

## References

(1) S. Yao, X. Zhang, H. Wang, H. Wang, X. Gan, Z. Wu, Y. Tian, Z. Pan and H. Zhou, *Dyes Pigments*, 2017, **145**, 152–159.

- (2) B. Jarzabek, B. Kaczmarczyk and D. Sęk, *Spectrochimica Acta Part A*, 2009, **74**, 949–954.
- (3) S. Afzal, A. Gul and Z. Akhter, *J. Inorg. Organomet. Polym.*, 2014, **24**, 321–332.
- (4) S. Nevejans, N. Ballard, M. Fernández, B. Reck, J. M. Asua, *Polymer*, 2019, **166**, 229–238
- (5) S. Nevejans, N. Ballard, I. Rivilla, M. Fernández, A. Santamaria, B. Reck and J. M. Asua, *Eur. Polym. J.*, 2019, **112**, 411–422.